EFFECTS OF OPERATING CONDITIONS AND SUPPLY HOLE DIAMETER ON THE PERFORMANCE OF RECTANGULAR AEROSTATIC BEARING

Sadek Z. Kassab, Elsayed M. Noureldeen and Medhat A. Shawky
Mechanical Engineering Department, Faculty of Engineering,
Alexandria University, Alexandria, Egypt.

ABSTRACT

The present study is an experimental investigation of the performance characteristics of externally pressurized rectangular recessed gas bearing operating under different working conditions. It includes the measurements of pressure, load carrying capacity, and mass flow rate. The experiments covered a wide range of film thicknesses and supply pressures. In addition, pads of different supply hole diameter were used. The results obtained from the present investigation show that the effect of varying the supply hole diameter on bearing performance is significant. Increasing the supply hole diameter to bearing length ratio has the effect of increasing the recess pressure and load carrying capacity. Further, as the supply pressure and/or film thickness increases the dimensionless load carrying capacity decreases and the lubricant mass flow rate increases.

Keywords: Aerostatic bearing, Supply hole.

1. INTRODUCTION

Lubrication plays a most vital role in our great and complex civilization. It keeps the surfaces apart by the lubricating fluid and the friction that results is due to viscous shear in the fluid, which is usually many times less than dry friction. Bearings are classified, according to the manner in which the fluid pressure is developed, to three general classes: dynamic or self acting, squeeze film and hydrostatic or externally pressurized types.

The hydrostatic or externally pressurized bearings develop load capacity due to lubricant flow from an external supply (pump or compressor). The essential property of this type being that the load carrying surface is floated irrespective of relative motion between bearing surfaces. Because of their many advantages, externally pressurized bearings are widely used for slow speed and in applications where precise separation under varying conditions must be maintained. On the other hand bearings are classified according to lubricant to gaseous and liquid bearings. The advantages of the gas bearing have results in numerous applications such as in measuring instruments, machine tools, detail drills, jet engines, and computer peripheral devices.

According to the wide scope of applications of externally pressurized gas bearing, a great deal of research work had been directed to this subject especially at the Mechanical Engineering Department, Alexandria University. A recent review concerning this programme is given by Kassab [1]. Experimentally, Shawky [2] and Salem and Shawky [3] investigated the effect of different parameters on the performance of rectangular air bearings. They concluded that the assumption of one dimensional flow is proper when the recess length approaches the bearing outer length. Introducing a recess, and/or step in the bearing surface has an increasing effect on the pressure depression following the inlet supply hole. In addition they found that rounding the supply hole has an improving effect on the pressure distribution and the load carrying capacity on the expense of the increase in the mass flow rate. It is important to note that Shawky [2] and Salem and Shawky [3] based their experimental work on constant recess pressure without considering the effect of hydraulic resistance and supply pressure when dealing with the effect of bearing geometry and dimensions.

On the other hand, Kassab [4] and Shawky and Kassab [5&6] investigated experimentally the performance of externally pressurized rectangular air bearing operating under constant supply pressure. Kassab [4] observed that the dimensionless pressure profile in the inlet zone of air bearing is characterized

with pressure depression. Meanwhile Shawky and Kassab [5] found that, for a rectangular gas bearing of specified supply hole diameter and recess length to outer length ratio, there is an optimum bearing width to length ratio that gives maximum dimensionless load carrying capacity and consumes minimum mass flow rate without any remarkable loss in the bearing stiffness.

Boffey et al i [7] concluded that for rectangular gas bearing, the effect of increasing the races length is to increase maximum load capacity and maximum bearing stiffness. In addition Boffey et al i[8] found that the effect of increasing the depth of the recess is to increase the load at a given film thickness.

Kandil [9] and Khalil et al [10] showed that for externally pressurized rectangular air bearing, and for the same operating conditions and bearing dimensions, the pressure distribution, load carrying capacity and lubricant mass flow rate for the elastic lined bearing are higher than that for the rigid bearing.

Shawky [11] used Kassab's [4] results to obtain an empirical formula which relates the maximum value of pressure recovered after depression with the outer supply pressure for different operating conditions and outer dimensions. Meanwhile, Kassab [1] compared the theoretical results obtained using Shawky's empirical equation with a sample of available experimental results and found a qualitative agreement. It is important to mention that the studies of Shawky [11] and Kassab [1] did not include the effect of varying the supply hole diameter on the bearing performance.

The aim of the present investigation is to study experimentally the effect of varying the supply hole diameter, along with the other operating conditions on the performance of externally pressurized rectangular air bearing. In addition, another objective of the present experimental study is to provide the researcher in the related area with experimental data that help them in improving the mathematical models and modifying the empirical correlations. This leads to a better understanding of the bearing performance and provides the designers with information close to the real performance.

2. EXPERIMENTAL SET-UP AND PROCEDURE

For measuring the pressure distribution, load carrying capacity, and mass flow rate of externally pressurized rectangular air bearing, at different supply pressures and different film thicknesses, a testing apparatus was designed and constructed. The experimental set-up, shown in Figure (1), consists of the apparatus, the hydraulic circuit, and measuring devices. The apparatus shown in Figure (2), consists of an aluminum frame, a cast iron base and the bearing. The bearing consists mainly of two elements which are the bed and the pad. The measurements were done for five different pads having supply hole diameter, d_o, to bearing outer length (L_o=120 mm) ratios of 0.0167, 0.020, 0.0225, 0.0250, and 0.0275. The other pad dimensions were kept constant as follows: recess width to outer width ratio (B_r/B_o) of 0.1, recess length to outer length ratio (L_r/L_o) of 0.9 and recess depth of ten times the maximum operating film thickness, i.e 500 μm.

The hydraulic circuit consists of the air compressor, the pipe line and the control system. Other details about the experimental set-up and apparatus can be found in Noureldeen [12].

The measurements necessary to carry out the experimental investigations were pressure, film thickness, load, and flowrate. The tapping holes on the bed were connected to the upper ends of mercury piezometer tubes 180 cm long each, branching from one header. In addition, two calibrated Bourdon gauges were used. The first was used to measure the pressure upstream of the rotameter and the other to measure the supply pressure. Film thicknesses were measured with three dial gauges of 1 μm division fitted into pad with there stems touching the bed surface to achieve uniform film thickness. A calibrated load ring of spring steel was used to measure the load exerted on pad by reading the deflection on the ring. The load was then obtained using a calibration curve.

A rotameter was used to measure the flow rate. The pressure and temperature were measured before the rotameter to determine the air density in order to calculate the mass flow rate. Two calibrated rotameters of different size were used to cover the different ranges of flow rate.

The regulating valve was used to adjust the supply pressure measured by the Bourdon gauge at the required value and the film thickness was readjusted. After recording the pressure the bed was moved 1 mm and the film thickness was readjusted and the pressure was recorded. The readings of the pressure distribution were recorded at five values of the film thickness (10, 20, 30, 40 and 50 μm), at different values of supply pressure (1.5, 2, 2.5, and 3 bar abs) for pads of different configurations.

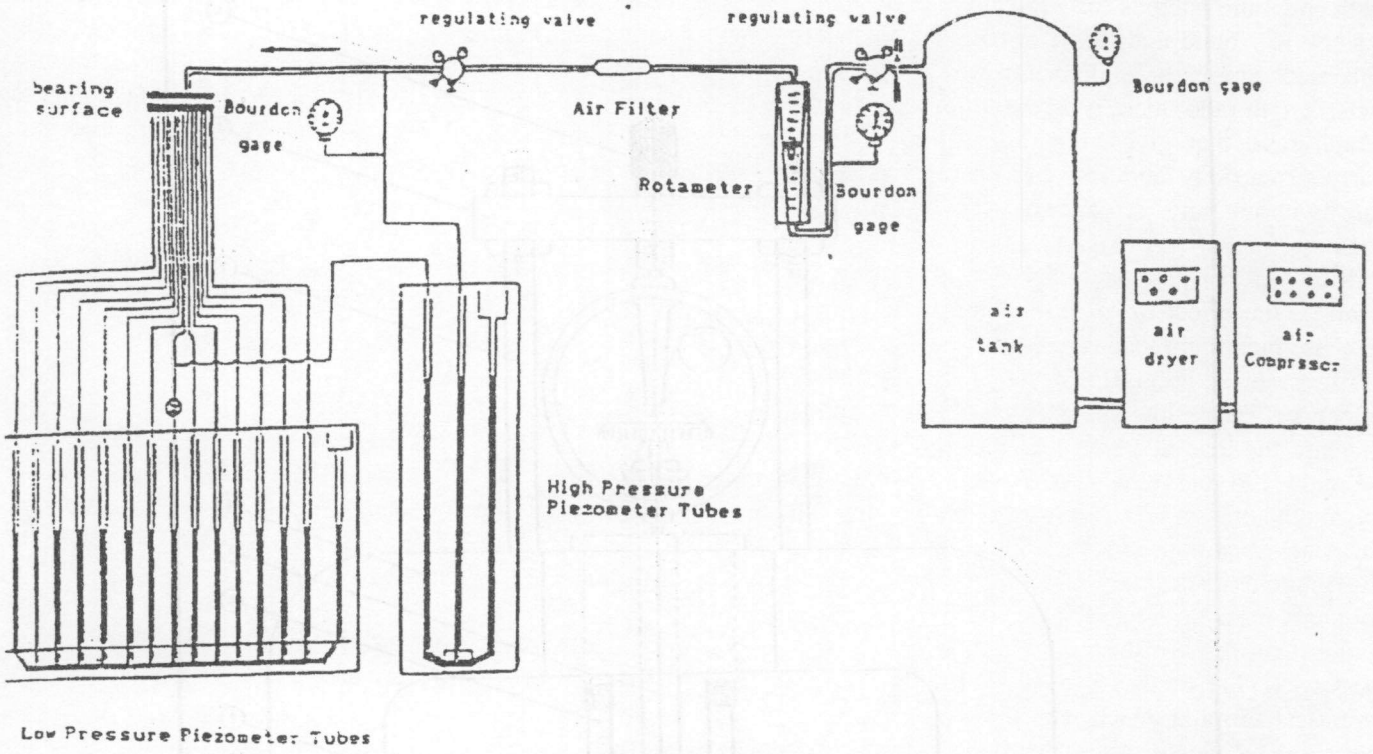

Fig.1 Experimental set-up

For each set of observation the following measurements were also recorded:

1. The reading of bourdon gauge indicating the supply pressure upstream of the pad.
2. The readings of the high pressure piezometer tubes.
3. The readings of the low pressure piezometer tubes.
4. The readings of the Bourdon gauge indicating the pressure upstream of the rotameter.
5. The reading of the rotameter.
6. The reading of dial gauge located inside the calibrated ring with vibrator.

From these observations, it was possible to calculate the load carrying capacity, the flow rate and the pressure distribution along the pads at different operating conditions. For each pad, the experiments were made for the prementioned film thickness, while supply pressure was kept constant. The procedure was repeated for other values of supply pressure for the same pad. After that, the pad was replaced with another one of different dimensions and same procedure was repeated.

To assert uncertainty of the experimental data the pressure distribution was obtained for a pad of width to outer length ratio $B_o/L_o = 2/3$ and the obtained results compared with the results of kassab [4] and were found in good agreement. In addition, for pad having $B_o/L_o = 5/6$ the pressure measurements were repeated three times at different days for supply pressure, $P_s = 2$ bar abs at three different film thickness H = 10, 30, and 50 μm. The obtained results show that the repeatability of data is good and the random error is small. This gives confidence on the data obtained and consequently throughout the present investigation, in case of repeating the data, only one run will be presented. Other details concerning the error analysis of the experimental data can be found in Noureldeen [12].

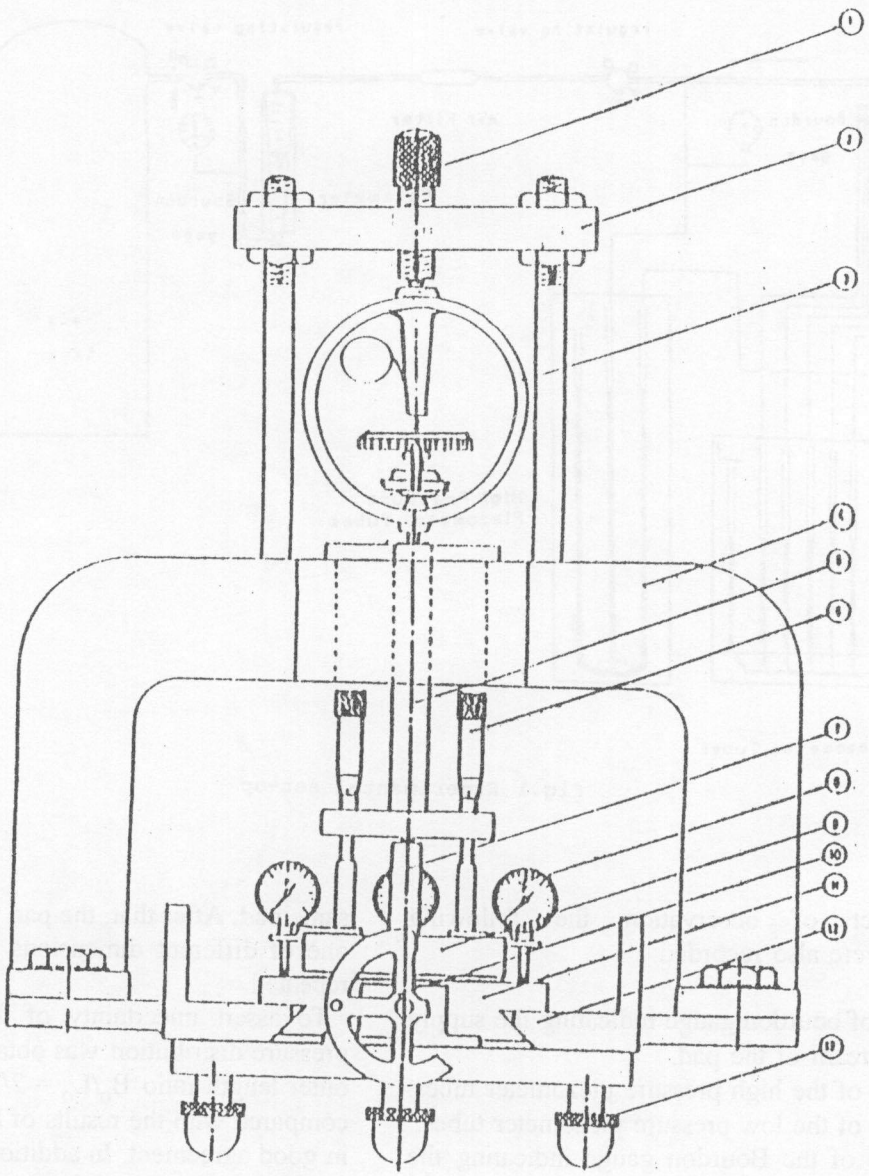

1- Calibrated Ring Holder.
2- Steel Supporting Beam.
3- Calibrated Ring.
4- Aluminum Frame.
5- Load Transmitting Shaft.
6- 3 Adjusting Micrometer Heads.
7- Centering Steel Bolt.
8- 3 Dial gauges.
9- Steel Pad.
10- Bed Driving Wheel.
11- Steel Bed.
12- Cast Iron Base.
13- 3 Levelling Screws.

Fig.2 Test apparatus

3. RESULTS AND DISCUSSION

The experimental results of pressure distribution, load carrying capacity and mass flow rate for externally pressurized stationary rectangular recessed air bearing are presented and discussed. Only the pads having $B_o/L_o = 5/6$ and $B_r/B_o = 0.1$, which gave the optimum bearing performance (maximum dimensionless load and minimum mass flow rate), are considered. In addition, the ratio between recess length to pad outer length, L_r/L_o, is kept constant at 0.9.

The pressure measurements will be presented first. They are presented in dimensionless form using the supply pressure. The dimensionless pressure are plotted versus the dimensionless distance from bearing centerline at different values of $2x/B_o$ from zero to 1.

The effect of varying the film thickness, H, from 10 μm to 50 μm at different values of supply pressure, P_s, from 1.5 bar abs. to 3.0 bar abs. and for two supply hole diameters, are presented in Figures (3) and (4), respectively. It is clear from these figures that for a certain film thickness, H, the first measured point for the dimensionless pressure (inlet pressure) is less than the supply pressure due to the pressure drop through the capillary resistance. At the entrance region the pressure drops first to a minimum value after that it then increases to a maximum value less than the inlet pressure. This phenomenon is called pressure depression. Within the bearing region $\frac{2B_r}{B_o} \leq \frac{2x}{B_o} \leq 1$ the pressure decreases until it reaches the atmospheric pressure at the bearing outer surface. Further, for a certain position, $2x/B_o$, as the film thickness, H, increases, the dimensionless pressure decreases, This is due to pressure depression, and entrance effects at the sharp edge supply hole. In addition as the film thickness increases, the inertia effect becomes more significant, causing more pressure drop. Moreover, the pressure results show that at the inlet region the effect of the pressure depression is more significant as the film thickness increases. It is important to note that Figures (3) and (4) show that the previous observations are true for all supply pressures and for all pads of different supply hole diameters.

The effects of varying the supply pressure on the dimensionless pressure distribution are shown in Figures (5) and (6). It is clear from these figures that as the supply pressure increases the dimensionless pressure decreases. This is due to the increase of the inlet pressure depression effect as the supply pressure increases. Further, Figures (5) and (6) show that the effect of supply pressure on the pressure distribution is more significant for higher film thicknesses than for the smaller ones.

The effects of varying the supply hole diameter, for different values of the bearing film thickness, H, and supply pressure, P_s, are presented in Figures (7) and (8). As the supply hole diameter ratio, d_o/L_o, increases, the pressure rises and the ratio between recess pressure and supply pressure increases. It can be stated that increasing the supply hole diameter to pad length ratio increases the recess pressure and improve the bearing performance. This is due to increasing the area of the supply hole that allows the large flow rate required for that bearing of small hydraulic resistance to flow into the bearing with relatively small velocity which decreases the separation effect which usually takes places at the entrance region.

On the other hand the results of the load carrying capacity presented in Figures (9) and (10) for different values of film thicknesses, supply pressures and supply hole diameters. Figure (9) shows the variation of the load with film thickness, H. For a certain value of supply pressure, P_s, as the film thickness increases the load decreases. This is in agreement with the pressure results shown previously in Figures (3) and (4). As the film thickness increases the pressure depression increases which results in a decrease in the pressure and consequently the load. Further, the rate of decrease of the load is higher for high supply pressure than the lower one.

Furthermore Figure (9) shows that, for a certain film thickness, as the supply pressure increases the load increases. This is physically correct because the load is always proportional to the pressure. Moreover, the above observations are the same for all bearings with various supply hole diameters as shown in Figure (9).

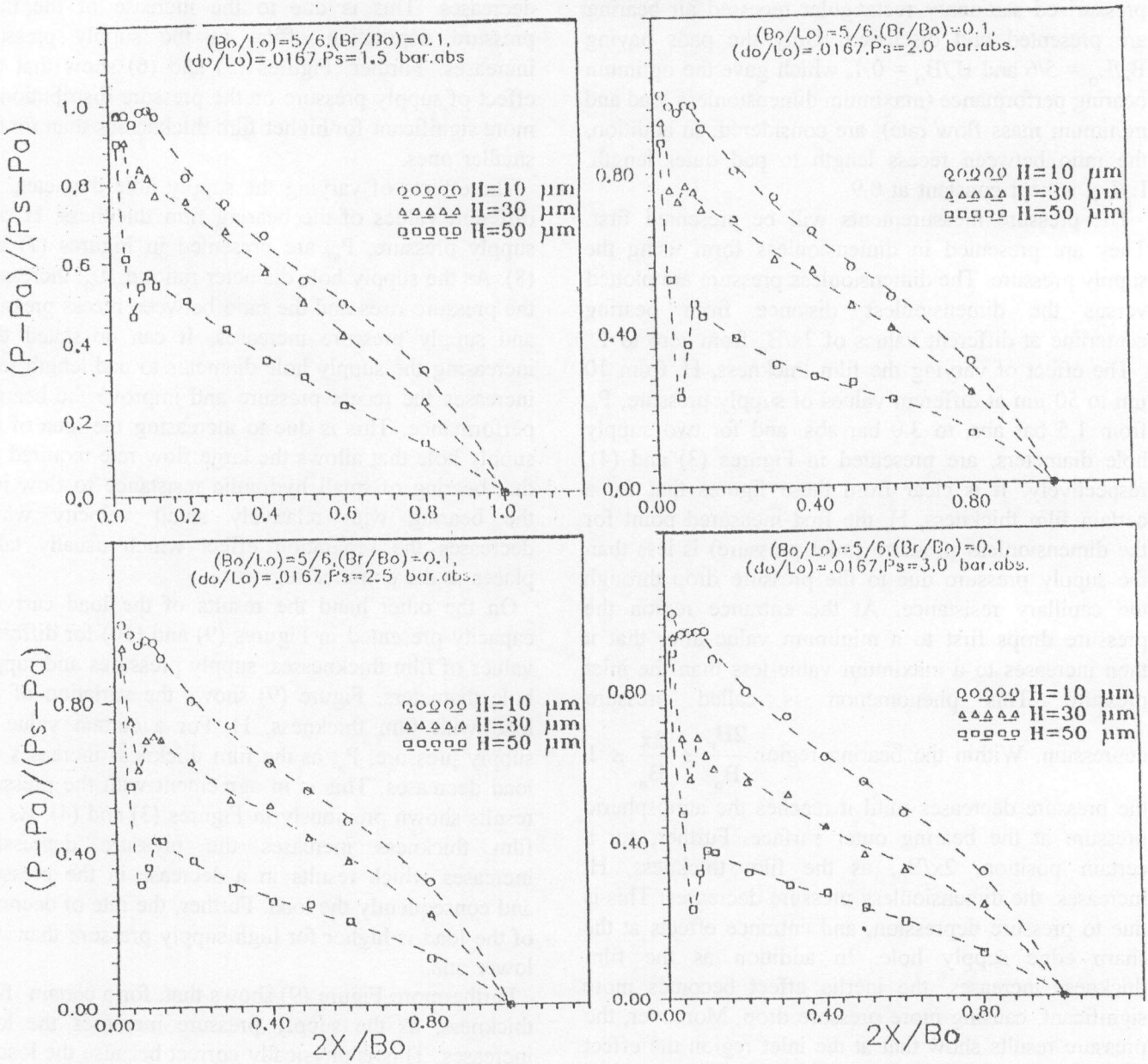

Fig.3 Effect of varying the film thickness, H, on the pressure distribution for d_o/L_o = 0.0167

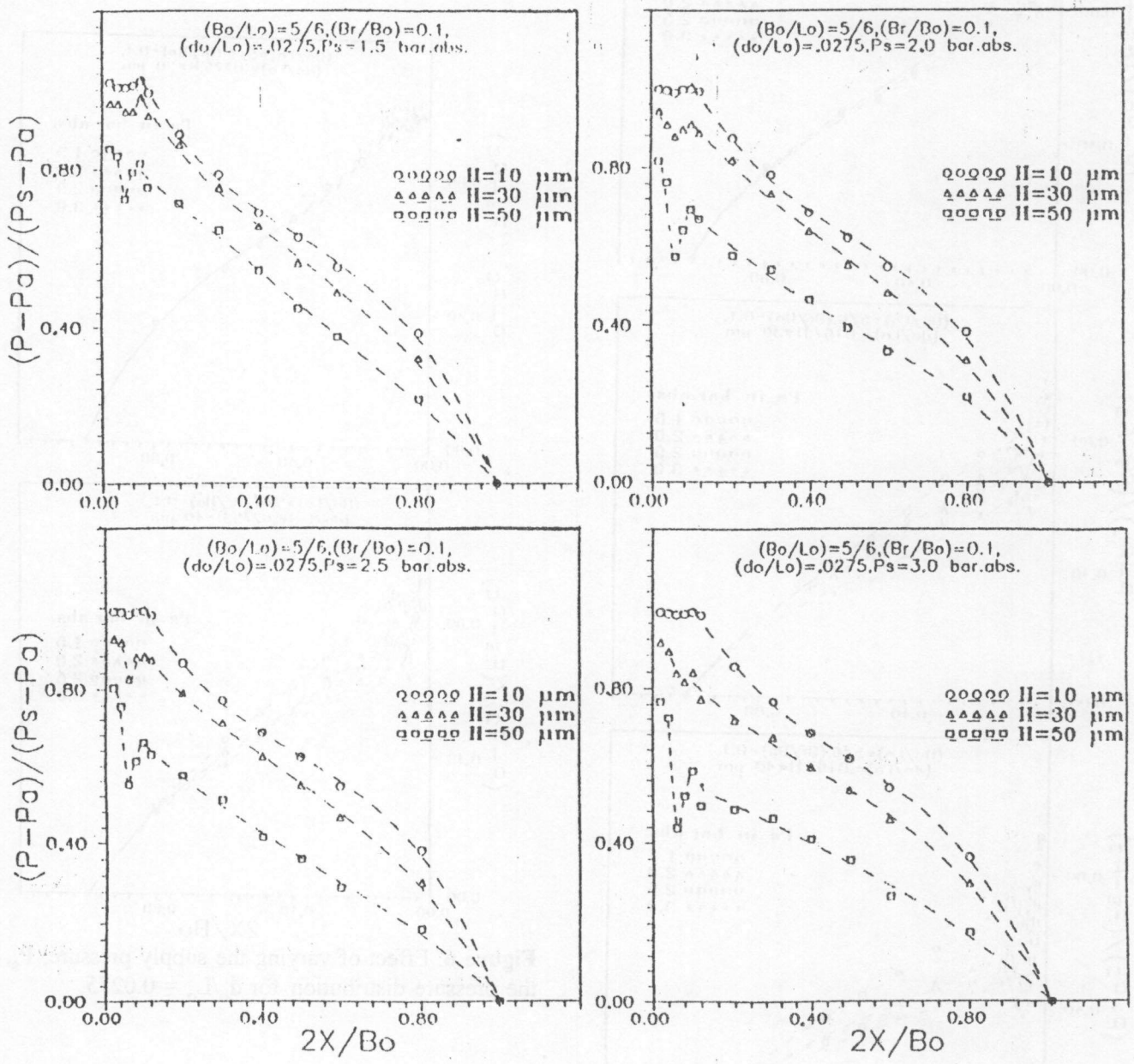

Fig.4 Effect of varying the film thickness, H, on the pressure distribution for d_o/L_o = 0.0275

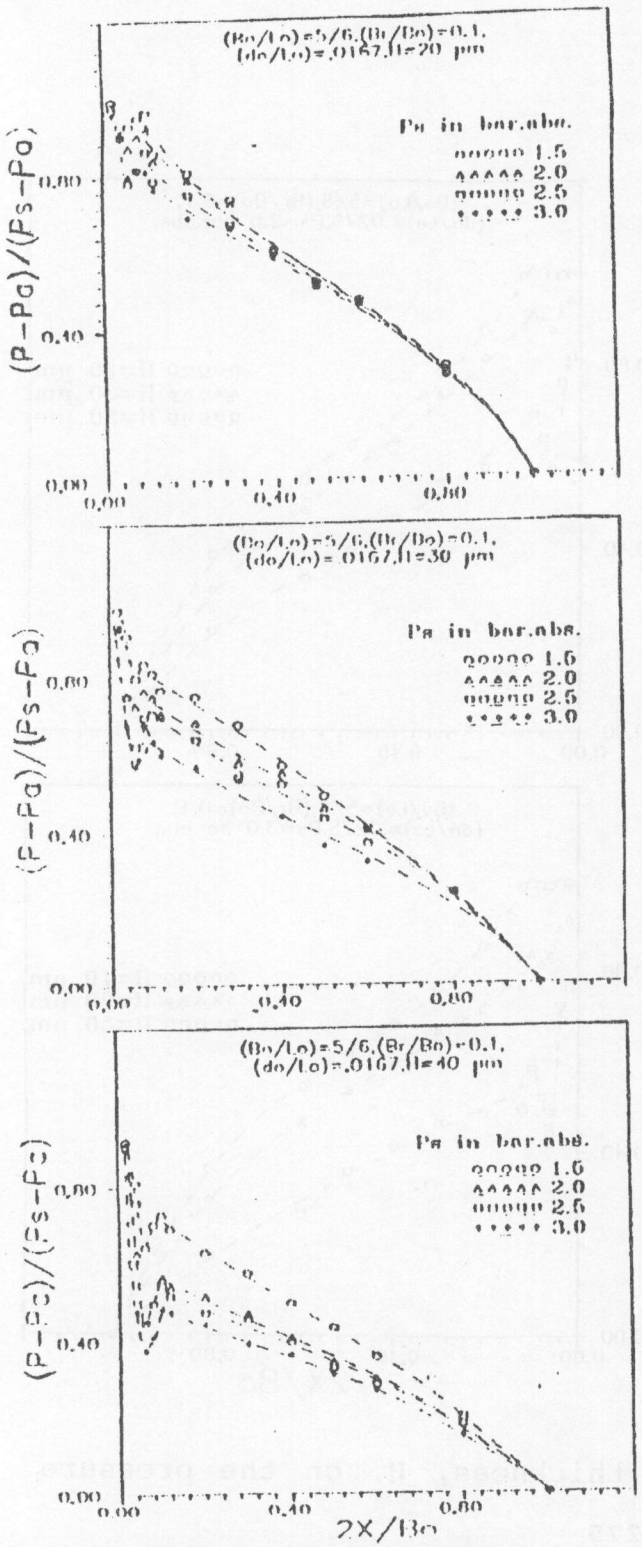

Figure 5. Effect of varying the supply pressure, P_s, on the pressure distribution for d_o/L_o =0.0167.

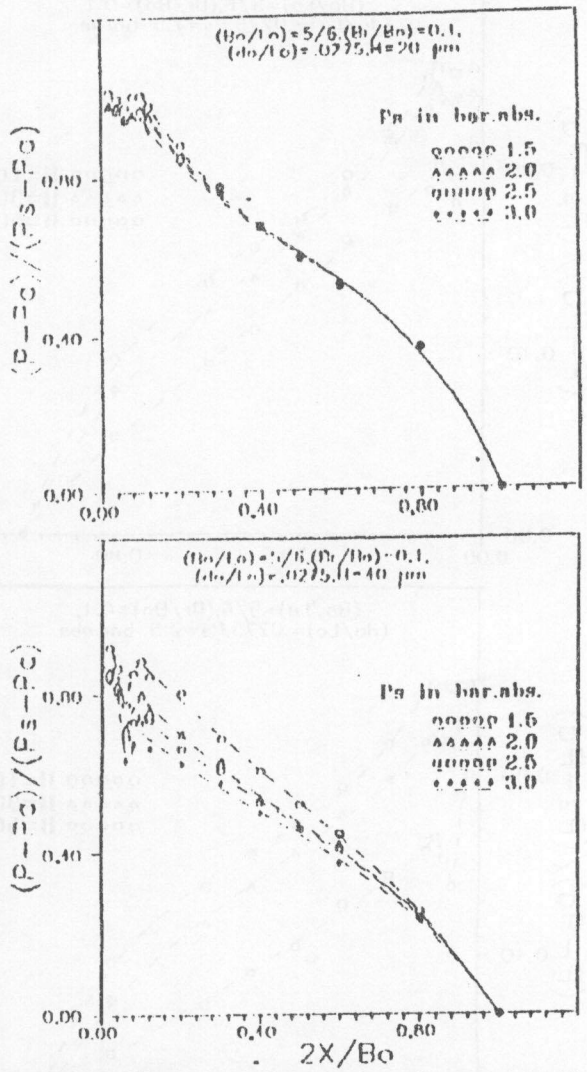

Figure 6. Effect of varying the supply pressure, P_s, on the pressure distribution for d_o/L_o = 0.0275.

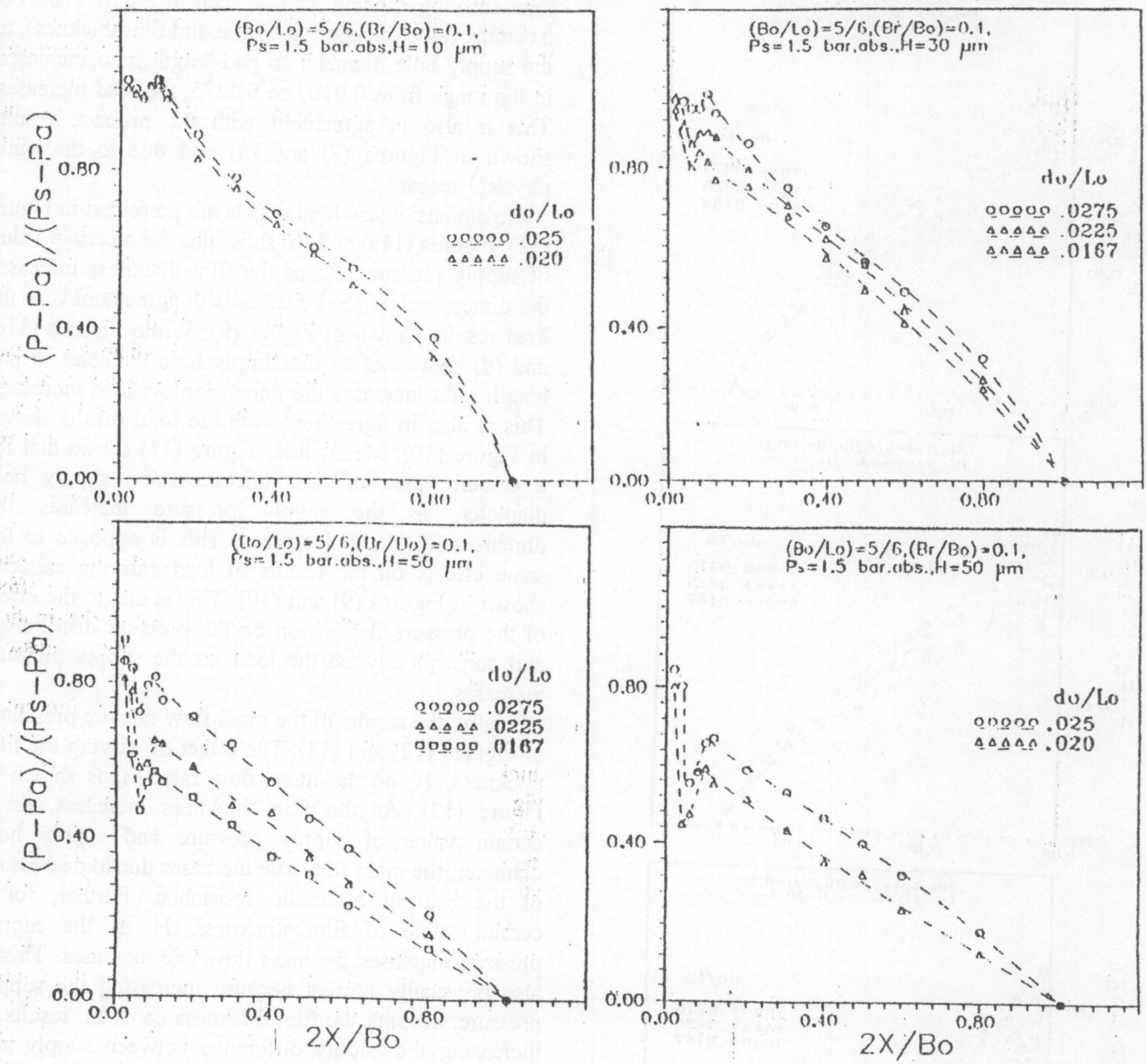

Fig.7 Effect of varying the dimensionless supply hole diameter, d_o/L_o, on the pressure distribution for P_s = 1.5 bar abs.

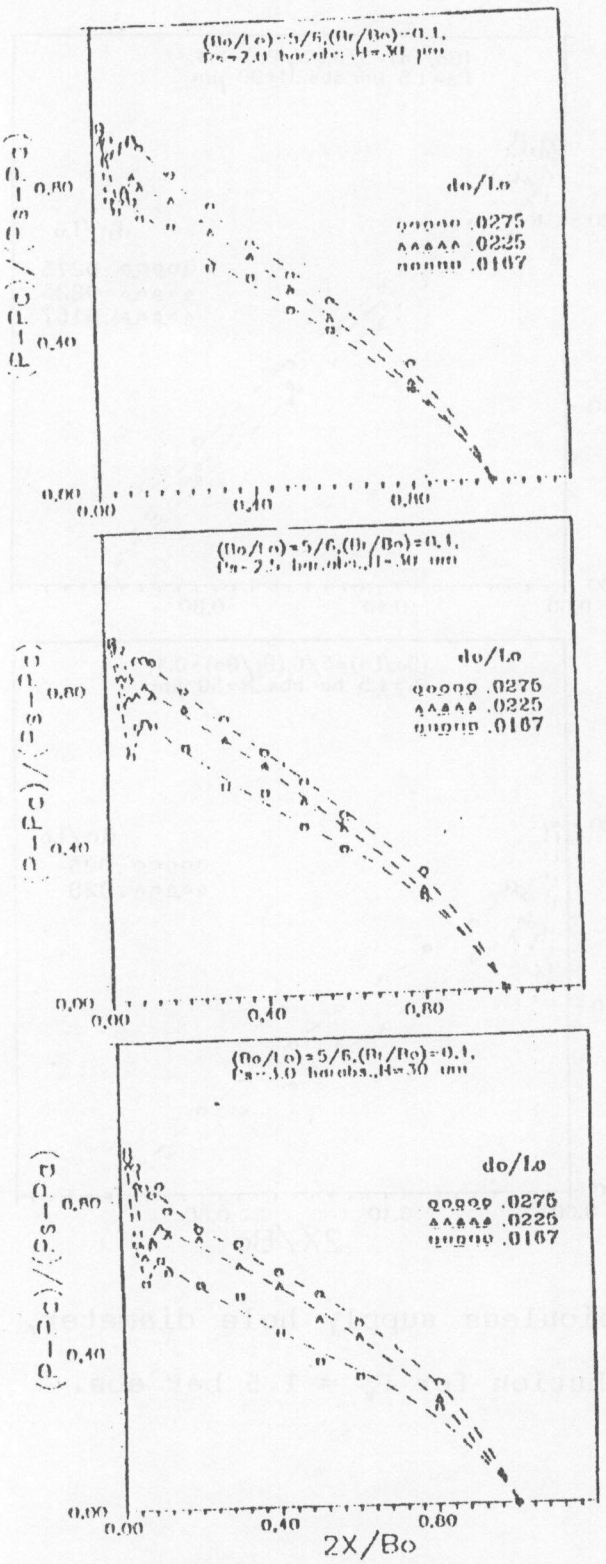

Figure 8. Effect of varying the dimensionless supply hole diameter, d_o/L_o on the pressure distribution for H= 30 μm.

The effect of varying supply hole diameter on the load carrying capacity can be seen in Figure (10). For a certain value of supply pressure and film thickness, as the supply hole diameter to pad length ratio increases, in the range from 0.0167 to 0.0275, the load increases. This is also in agreement with the pressure results shown in Figures (7) and (8) and due to the same physical reasons.

The dimensionless load results are presented in Figure (11). Figures (11a) and (b) show that for a certain value of supply pressure, P_s, as the film thickness increases the dimensionless load decreases in agreement with the load results shown in Figure (9). While Figures (11c) and (d) show that as the supply hole diameter to pad length ratio increases the dimensionless load increases. This is also in agreement with the load results shown in Figure (10). Meanwhile, Figure (11) shows that for a certain value of film thickness and supply hole diameter, as the supply pressure increases the dimensionless load decreases. This is apposite to the same effects on the results of load carrying capacity shown in Figures (9) and (10). This is due to the effect of the pressure depression on the pressure distribution and consequently on the load, as the supply pressure increases.

Finally, the results of the mass flow rate are presented in Figures (12) and (13). The effect of varying the film thickness, H, on the mass flow rate, M, is shown in Figure (12). As the film thickness increases, for a certain value of supply pressure and supply hole diameter, the mass flow rate increases due to decreasing of the bearing hydraulic resistance. Further, for a certain value of film thickness, H, as the supply pressure increases the mass flow rate increases. This is also physically correct because increasing the supply pressure, keeping the film thickness constant, results in increasing the energy difference between supply and exit sections consequently increasing the mass flow rate.

Figure (13) shows the effect of varying the supply hole diameter on the mass flow rate. As the supply hole increases the mass flow rate increases. In addition Figure (13) shows that for a certain value of d_o/L_u and H, as the supply pressure increases the mass flow rate increases. This is also due to the increase of the energy difference between the supply and exit sections.

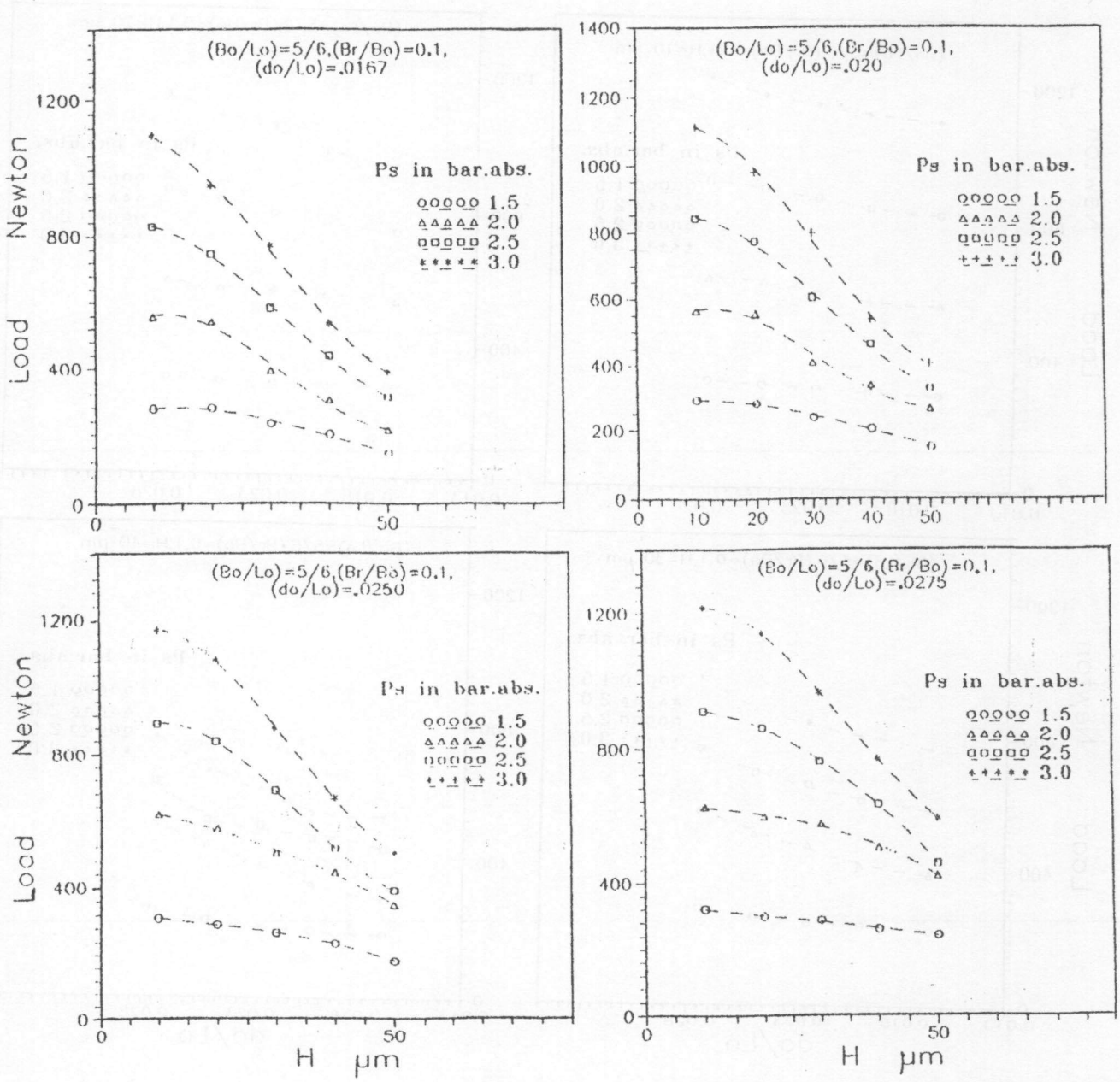

Fig.9 Variations of the load carrying capacity with the film thickness.

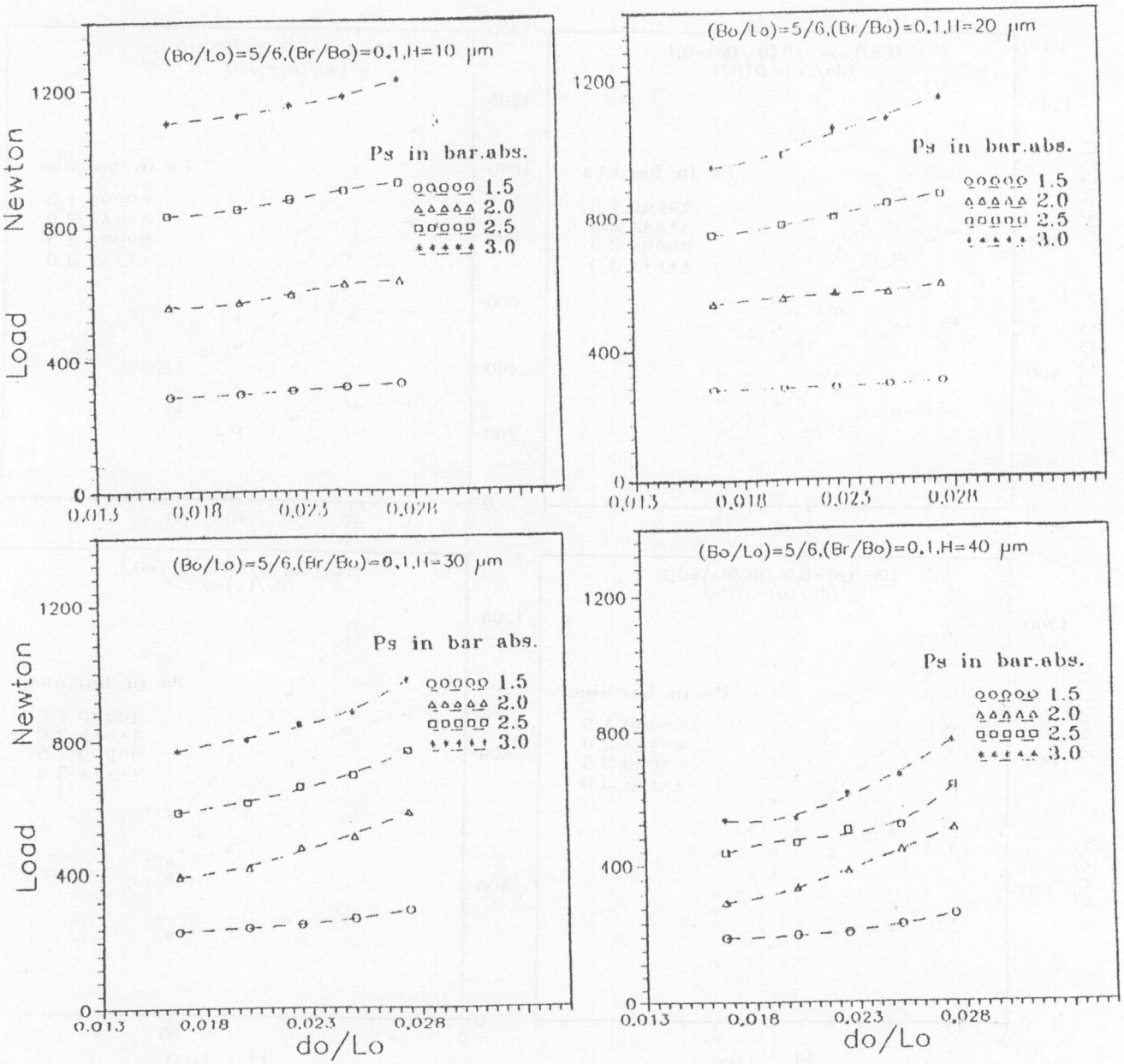

Fig.10 Variations of the load carrying capacity with the dimensionless supply hole diameter, d_o/L_o.

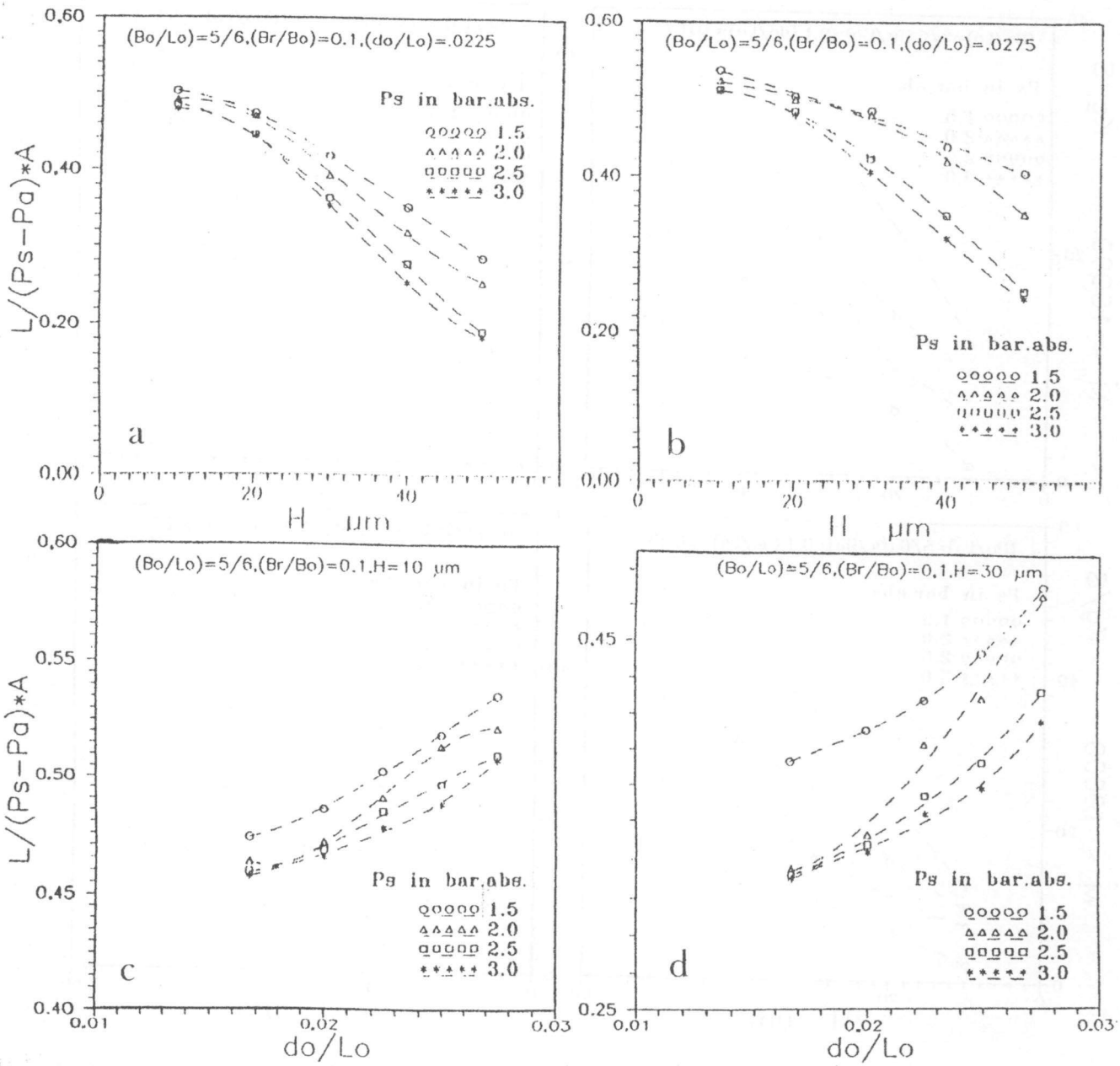

Fig.11 Variations of the dimensionless load with film thickness and dimensionless supply hole diameter.

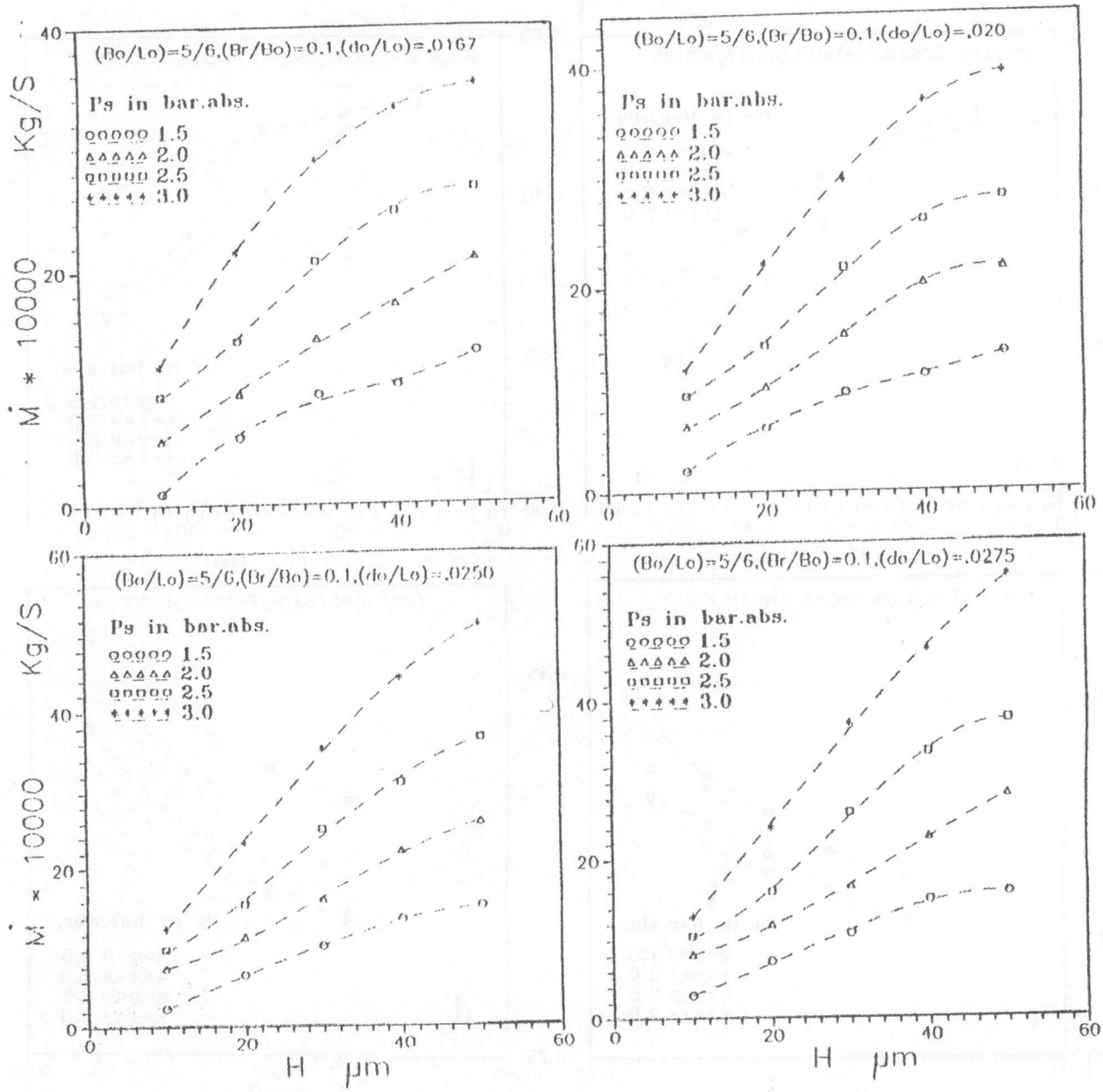

Fig.12 Variations of the mass flow rate, $\dot{M}$, with the film thickness.

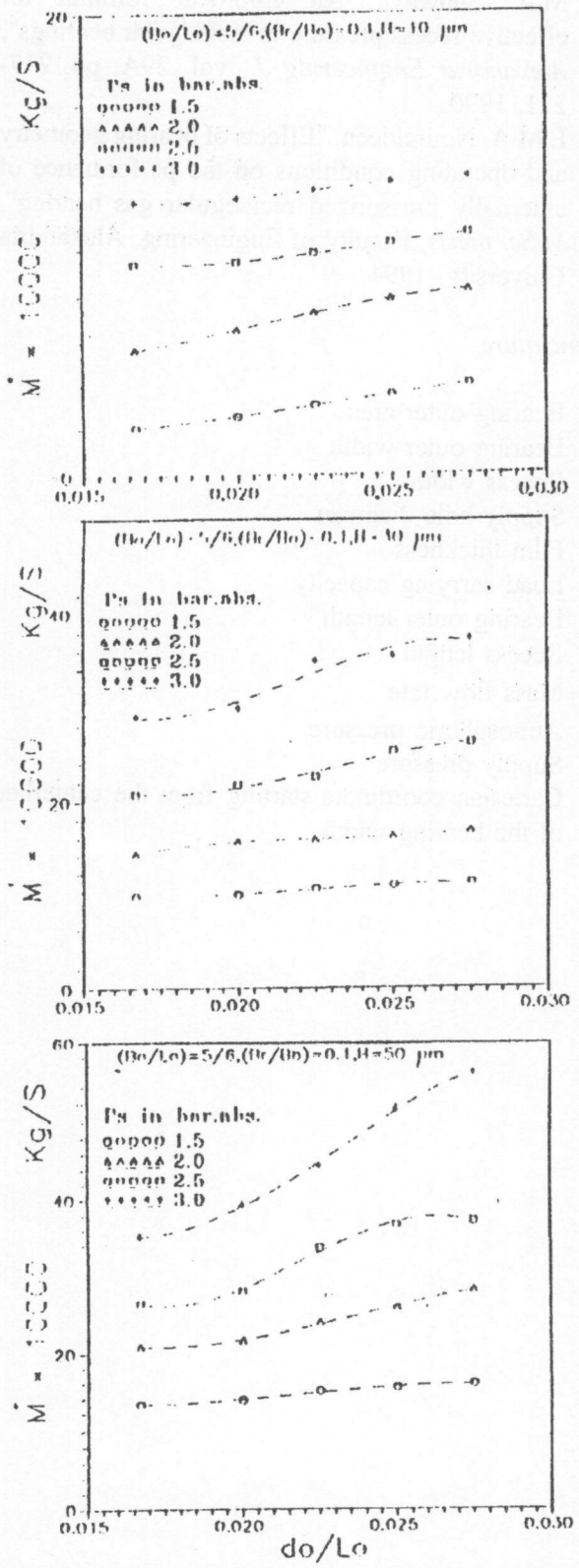

Figure 13. Variation of the mass flow rate, $\dot{M}$, with dimensionless supply hole diameter.

4. CONCLUSIONS

From the presented experimental results and associated discussion concerning the performance of externally pressurized rectangular air bearing under varying operating and geometric conditions the following concluding remarks can be drawn:

1. The dimensionless pressure profiles drop as the film thickness and/or the supply pressure increases.
2. The bearing load carrying capacity increases by decreasing film thickness and/or increasing supply pressure.
3. The dimensionless load decreases by increasing the film thickness and/or supply pressure.
4. The lubricant mass flow rate increases by increasing the film thickness and/or supply pressure.
5. Increasing the supply hole diameter to the pad outer length ratio improves the bearing performance as it raises the dimensionless pressure distribution and increases the load carrying capacity.
6. Increasing the supply hole diameter to the pad outer length ratio increases the lubricant mass flow rate.

REFERENCES

[1] S.Z. Kassab, "Performance of an externally pressurized rectangular gas bearing under constant effective recess pressure", *Tribology International*, vol. 27, pp. 159-167, 1994.

[2] M.A. Shawky, "Analysis and applications of gas bearings", *Ph.D. thesis*, Faculty of Engineering, Alexandria University, 1976.

[3] E.A. Salem and M.A. Shawky, An experimental investigation into the performance of externally pressurized rectangular air bearings, *Wear*, vol. 50, pp. 237-257, 1978.

[4] S.Z. Kassab, "Gas bearings", *M.Sc. thesis*, Faculty of Engineering, Alexandria University, 1980.

[5] M.A. Shawky and S.Z. Kassab, "Experimental Optimization of externally pressurized rectangular gas bearings dimensions", *Bulletin of the Faculty of Engineering*, Alexandria University, vol. 20, pp. 205-225, 1981.

[6] M.A. Shawky and S.Z. Kassab, "Performance Characteristics of externally pressurized rectangular gas bearing compensated with orifice

restrictor", *Bulletin of the Faculty of Engineering*, Alexandria University, vol. 20, pp. 227-248, 1981.

[7] D.A. Boffey, M. Waddell and J.K. Deardent, 'A theoretical and experimental study into the steady - state performance characteristics of industrial air lubricated thrust bearings", *Tribology International*, vol. 18, pp. 229-233, 1985.

[8] D.A. Boffey, A.A. Barrow and J.K. Deardent, "Experimental investigation into the performance of an aerostatic industrial thrust bearing", *Tribology International*, vol. 18, pp. 165-168, 1985.

[9] H.A. Kandil, "Optimization and performance improvements of externally pressurized rectangular gas bearings", *M.Sc. thesis*, Faculty of Engineering, Alexandria University, 1987.

[10] M.F. Khalil, M.A. Shawky and H.A. Kandil, "Elastohydrostatic lubrication of externally pressurized rectangular gas bearing: Experimental verification", *Presented at the Egyptian Society of Tribology, First Tribology conference*, 20-21 December, Cairo, Egypt, 1989.

[11] M.A. Shawky, "An empirical formula for effective recess pressure in rectangular bearings", *Alexandria Engineering J.*, vol. 29A, pp. 217-221, 1990.

[12] E.M.A. Noureldeen, "Effects of bearing geometry and operating conditions on the performance of externally pressurized rectangular gas bearing", *M.Sc. thesis*, Faculty of Engineering, Alexandria University, 1994.

Nomenclature

A	Bearing outer area
B_o	Bearing outer width
B_r	Recess width
d_o	Supply hole diameter
H	Film thickness
L	Load carrying capacity
L_o	Bearing outer length
L_r	Recess length
$\dot{M}$	Mass flow rate
P_a	Atmospheric pressure
P_s	Supply pressure
x	Cartesian coordinate starting from the centerline of the bearing width.